

## Adsorption and Decomposition of Hydrazine on Metal Films of Iron, Nickel, and Copper

Yousif K. Al-Haydari, Jalal Mohammed Saleh,\* and Mohammed H. Matloob

Department of Chemistry, College of Science, University of Baghdad, Baghdad, Jadiriya, Republic of Iraq  
(Received: September 10, 1984)

The interaction of hydrazine with evaporated metal films of Fe, Ni, and Cu has been investigated in the temperature range 243–393 K. Dissociative chemisorption of hydrazine occurred on Fe and Ni films at 243 K with liberation of  $\text{NH}_3$ ,  $\text{N}_2$ , and  $\text{H}_2$  gases. Adsorption on Cu film at the same temperature was molecular and a significant fraction of the adsorption was reversible. Two different mechanisms have been suggested for the adsorption and the subsequent formation of the decomposition products. Ammonia was the main gaseous product of hydrazine decomposition on the films at all temperatures. The desorption of the products was more extensive in the case of Ni film as compared with the other two metals. The activation energy ( $E_a$ ) of hydrazine adsorption as well as the preexponential factor ( $A$ ) in the rate equation remained independent of the extent of adsorption. The relationship which was found to exist between the values of  $\log A$  and those of  $E_a$  indicated the operation of a compensation effect in the hydrazine adsorption on the films. Copper film was found to have a greater capability for hydrazine adsorption than the other two films. The geometric requirements for an appropriate hydrazine adsorption on this metal are probably more satisfied than on the other two metals.

### Introduction

The catalytic decomposition of hydrazine is important because of its wide range of applications;<sup>1</sup> gas generation, fuel cells, and microrockets for artificial satellites are only few such applications. Moreover, the decomposition of hydrazine on certain metals such as iron is of particular interest for the understanding of the mechanism of ammonia synthesis.<sup>2</sup> The adsorption and reaction of hydrazine has been extensively studied on various pure metals and supported metal catalysts<sup>3</sup> but the mechanism of the reactions is not yet clearly understood.<sup>3,4</sup>

The object of the present study was to follow the adsorption and the decomposition of hydrazine on metal films of Fe, Ni, and Cu over the temperature range 243–393 K. The approach was to examine the catalytic characteristics of these metals under clean surface conditions and to obtain mass-spectrometric data regarding the extent of the various decomposition products throughout the reaction. No such work has been previously reported.

### Experimental Section

The apparatus consisted of two parts,<sup>4,5</sup> the first, for gas handling, capable of ultimate pressures of  $10^{-5}$  N m<sup>-2</sup>, and the second was a bakeable ultrahigh vacuum system capable of ultimate pressures of  $\leq 10^{-7}$  N m<sup>-2</sup>. Evacuation of each part was affected by two three-stage mercury diffusion pumps backed by a Speedivac type oil rotary pump. Films of iron, nickel, and copper were prepared from metal wires, 0.5 mm in diameter, which were spectroscopically standardized samples obtained from Johnson Matthey and Co. Ltd. Iron and nickel films were prepared from filaments by evaporation on to the glass walls of the adsorption vessel, 240-cm<sup>3</sup> capacity, maintained at 78 K. With copper, a known length (~5 cm) of copper wire was supported on a tungsten coil, prepared from 0.2-mm tungsten wire, and the latter was heated electrically. The tungsten coil was first degassed in the absence of copper wire, and the same coil was used for up to two evaporations, thereby keeping contamination to a minimum.

The apparatus was outgassed for a minimum of 8 h and the filaments were heated to as high a temperature as possible without film formation for a similar period. Iron and nickel filaments were reduced in pure hydrogen about 1300 K before degassing. During the deposition of the films the reaction vessel was maintained open to the pumps and the pressure was always  $< 10^{-6}$  N m<sup>-2</sup>. The films

were presintered before use by heating in vacuo for 1 h to a temperature at least as high as that to be used in the experiment.

Hydrazine of 97% purity was obtained from Fluka, the main impurity being water. The water content of hydrazine was reduced to 1% by distillation in the presence of potassium hydroxide. The gas was passed over a trap maintained at 243 K before use. Krypton was obtained from British Oxygen Co. in sealed glass bulbs (>99% pure) and the gas was further purified before use. Ammonia, nitrogen, and hydrogen gases which were used in calibration experiments were >99.5% pure; the mass-spectrometric analysis indicated that these gases were completely free of H<sub>2</sub>O. Furthermore, all the gases were passed to the reaction system via a trap which was maintained at 195 K.

After the film was prepared and annealed, the general procedures for determining the surface area with krypton and for subsequent adsorption experiments were similar to those described previously.<sup>4-7</sup> Calibration experiments with hydrazine showed that negligible adsorption and decomposition occurred on the glass walls of the reaction vessel. At the end of each run the apparatus was usually brought back to room temperature, the cold traps being removed first and, thereafter, a final mass-spectrometric analysis was performed. It was thus possible to check that no condensable gases were present in the cold traps.

The reaction vessel was coupled to a Quadravac 200 mass-spectrometer partial pressure gauge, obtained from Leybold-Heraeus, which operated on the quadrupole principle and covered the mass range 1–200 amu. The mass spectrometer was combined with a pressure converter which could reduce the gas pressure under investigation to  $< 10^{-1}$  N m<sup>-2</sup> without influencing its composition. The gauge head of the mass spectrometer for ion detection was supplemented by a Faraday cup for partial analysis down to  $10^{-6}$  N m<sup>-2</sup>.

Cracking patterns were determined with the Quadravac for all molecules relevant to the investigation. These included N<sub>2</sub>H<sub>4</sub>, NH<sub>3</sub>, N<sub>2</sub>, H<sub>2</sub>, H<sub>2</sub>O, and O<sub>2</sub>. The cracking patterns (Table I) were determined by measuring the peak heights at over 10 different pressures for each gas, expressing them as a percentage of the largest peak, and the average was calculated for each gas.

The mass-spectrometric data were analyzed for selected  $m/e$  peaks of the gas mixture by setting up and solving a set of simultaneous linear equations using matrix inversion technique.<sup>8-11</sup>

- (1) J. P. Contour and G. Ponnetier, *J. Catal.*, **24**, 434 (1972).
- (2) J. Block and G. Schulz-Ekloff, *J. Catal.*, **30**, 327 (1973).
- (3) M. Grunze, *Surf. Sci.*, **81**, 603 (1979).
- (4) D. Al-Mawlawi and J. M. Saleh, *J. Chem. Soc., Faraday Trans. 1*, **77**, 2965 (1981).
- (5) D. Al-Mawlawi and J. M. Saleh, *J. Chem. Soc., Faraday Trans. 1*, **77**, 2977 (1981).

- (6) J. M. Saleh, *Trans. Faraday Soc.*, **64**, 796 (1968).
- (7) J. M. Saleh, *J. Chem. Soc., Faraday Trans. 1*, **68**, 1520 (1972).
- (8) A. P. Gifford, S. M. Rock, and D. J. Comaford, *Anal. Chem.*, **21**, 1026 (1949).
- (9) E. G. Daigle and H. A. Young, *Anal. Chem.*, **24**, 1190 (1952).
- (10) C. Kemball, *Adv. Catal.*, **11**, 223 (1959); *Proc. R. Soc. London, Ser. A*, **207**, 539 (1951).
- (11) L. F. Hamilton, S. G. Simpson, and D. W. Ellis, "Calculations of Analytical Chemistry", McGraw-Hill, New York, 1969, pp 351–354.

TABLE I: Cracking Patterns for Relevant Molecules\*

gas	m/e											
	1	2	14	15	16	17	18	28	29	30	31	32
N <sub>2</sub> H <sub>4</sub>	68.87	12.58	2.64	16.55	24.5			100	14.56	15.89	21.18	60.92
NH <sub>3</sub>	3.4	8.9	7.1	76.1	100.0			48.6		11.1		
N <sub>2</sub>			20.0					100.0		9.5		
H <sub>2</sub>	2.0	10.00			1.8	21.5	100.0					
H <sub>2</sub> O					13.5							
O <sub>2</sub>												100.0

\*Determined with a Quadruvac 200 Leybold-Heraeus mass spectrometer.

TABLE II: Interaction of Hydrazine with Metal Films of Fe, Ni, and Cu at 243 K\*

film	V <sub>Kr</sub>	V <sub>1</sub>	θ	V <sub>H<sub>2</sub></sub>	V <sub>N<sub>2</sub></sub>	V <sub>NH<sub>3</sub></sub>
Fe	129.3	77.5	0.60	0.15	6.20	17.8
Ni	45.0	33.0	0.73	8.00	9.70	18.4
Cu	3.0	4.6	1.5			

\*V<sub>H<sub>2</sub></sub>, V<sub>N<sub>2</sub></sub>, and V<sub>NH<sub>3</sub></sub> were respectively the volumes of H<sub>2</sub>, N<sub>2</sub>, and NH<sub>3</sub> gases evolved. All the volumes were expressed in mm<sup>3</sup> at STP.

The partial pressure of each component was then computed from the uncorrected partial pressure and the appropriate sensitivity factor.

The volumes of the different parts of the apparatus were calibrated by sharing experiments, using each gas in turn and the volume of a McLeod-gauge as a standard volume. The volume of the McLeod gauge was calibrated with water.

#### Results

**Extent of Adsorption.** The volume of hydrazine taken up in the adsorption was calculated from sharing experiments in which the effective volume of the reaction vessel was determined as a function of the gas pressure in the presence and absence of the metal film; it was thus independent of thermomolecular flow. The uptake which was expressed in terms of a pressure at room temperature in a constant volume was converted into mm<sup>3</sup> at STP; this was denoted V<sub>1</sub>.

The extent (θ) of hydrazine adsorption on each film was expressed as

$$\theta = V_1 / V_{Kr} \quad (1)$$

where V<sub>Kr</sub> was the volume (mm<sup>3</sup> at STP) of the krypton monolayer on the film surface which was determined from the krypton adsorption isotherm at 78 K before the admission of hydrazine doses. Each cubic millimeter of the adsorbed krypton corresponded to an area of 52.4 cm<sup>2</sup>, assuming a cross-sectional area of 0.195 nm<sup>2</sup> for the krypton atom.

The rate of hydrazine adsorption was calculated from the volume of gas uptake (mm<sup>3</sup>) per unit time (s<sup>-1</sup>) per unit area (cm<sup>2</sup>) of the film surface. The adsorbed volume of the gas was also converted into the number of hydrazine molecules adsorbed, thus enabling the rate of adsorption to be estimated in terms of molecules cm<sup>-2</sup> s<sup>-1</sup>.

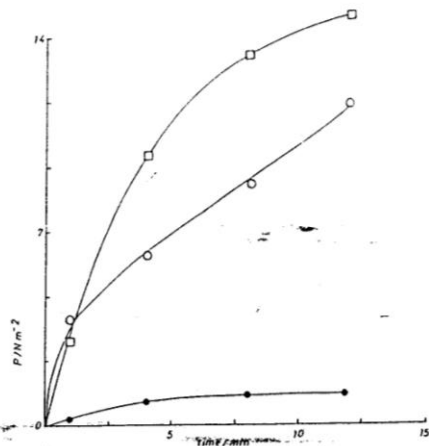
The initial mass-spectrometric analysis of gas composition could be performed in <1 min after the admission of hydrazine to the reaction system. A full mass spectrum of the gas phase could only be obtained in about 3 min, thus limiting the time interval for two successive mass-spectrometric analyses to ≈3 min.

**Adsorption and Decomposition. Iron.** Fast (<1 min) dissociative chemisorption of hydrazine occurred on Fe film at 243 K and the adsorption was accompanied by the evolution of N<sub>2</sub> and NH<sub>3</sub> gases; NH<sub>3</sub> was the major gaseous product. The extent of adsorption at this temperature corresponded to θ = 0.6, after which the rate of hydrazine uptake fell below 10<sup>-4</sup> mm<sup>3</sup> s<sup>-1</sup> cm<sup>2</sup>. Table II gives the data concerning the amount of gas uptake on Fe film at 243 K as well as of the gaseous products subsequent to hydrazine decomposition on the film surface.

The rate of hydrazine uptake increased as the temperature of the film was raised successively to 393 K; ammonia remained the main gaseous decomposition product at all temperatures below 393 K. Appreciable amounts of hydrogen appeared at 273 K but

TABLE III: Composition of Gaseous Products throughout the Hydrazine Interaction with Fe, Ni, and Cu Films at Several Temperatures

film	temp/K	NH <sub>3</sub> /%	N <sub>2</sub> /%	H <sub>2</sub> /%
Fe	273	68.72	24.4	6.83
	303	60.58	26.29	13.10
	333	66.43	21.75	11.80
	363	60.56	22.07	17.47
	393	40.78	3.79	55.92
Ni	273	56.23	26.13	17.63
	303	63.20	23.15	13.64
	333	71.10	25.59	3.30
	363	76.03	19.97	3.98
	393	81.86	18.13	0.10
Cu	273			
	303	75.60	18.75	5.62
	333	72.63	22.93	4.58
	363	69.49	27.23	3.25
	393	69.56	27.34	3.10

Figure 1. Liberation of gases throughout the interaction of hydrazine with iron film at 393 K: ●, N<sub>2</sub>; ○, NH<sub>3</sub>; □, H<sub>2</sub>.

it was present in smaller amounts than those of NH<sub>3</sub> and N<sub>2</sub>. Hydrogen became the main gaseous product at temperatures ≥393 K; the pressure of N<sub>2</sub> gas at this stage decreased considerably as indicated in Table III. It has been found that the total gas pressure at any temperature below 393 K increased to twice that of the hydrazine which disappeared. Figure 1 shows the decomposition of hydrazine on a Fe film at 393 K.

**Nickel.** Hydrazine adsorption on Ni at 243 K occurred in a manner similar to that on Fe. The maximum extent of hydrazine adsorption at this temperature on Ni film corresponded to θ = 0.73 (Table II) under a hydrazine pressure of 6 N m<sup>-2</sup>; the rate of adsorption at this stage was 10<sup>-3</sup> mm<sup>3</sup> s<sup>-1</sup> cm<sup>-2</sup>. The main

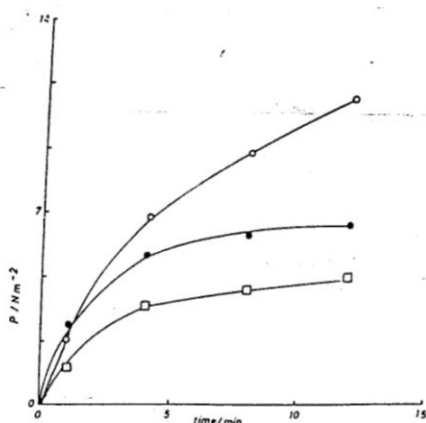


Figure 2. Evolution of gaseous products subsequent to hydrazine adsorption on Ni film at 273 K. Symbols as in Figure 1.

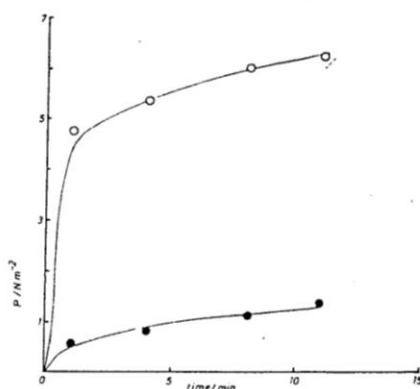


Figure 3. Desorption of gaseous products throughout the adsorption and decomposition of hydrazine on Cu film at 333 K. Symbols as in Figure 1.

gaseous product was again  $\text{NH}_3$  and its amount was comparable with the sum of both  $\text{H}_2$  and  $\text{N}_2$  gases.

Hydrazine adsorption on Ni film above 243 K took place at a higher rate. Hydrogen evolution became less pronounced as the temperature exceeded 303 K and a similar behavior, though to a lesser extent, was observed with  $\text{N}_2$  above 333 K;  $\text{NH}_3$  remained the major gaseous product of the decomposition (Figure 2). Table III gives the percentage of each of the gaseous decomposition products resulting from dissociative adsorption of hydrazine on Ni film. The rate of hydrazine adsorption above 293 K became fast with the main gas product being  $\text{NH}_3$ . The total gas pressure at any temperature increased as the pressure of hydrazine decreased.

**Copper.** Adsorption of hydrazine on Cu at 243 K was very fast (<1 min) and continued until  $\theta$  was 1.5 after which the hydrazine uptake proceeded at a rate of  $10^{-5} \text{ mm}^3 \text{ s}^{-1} \text{ cm}^{-2}$ . No gaseous product appeared at any stage subsequent to hydrazine adsorption on the film at this temperature (Table II). Some 20% of the adsorption was reversible which could be removed on pumping at the same temperature or on warming the film to 273 K.

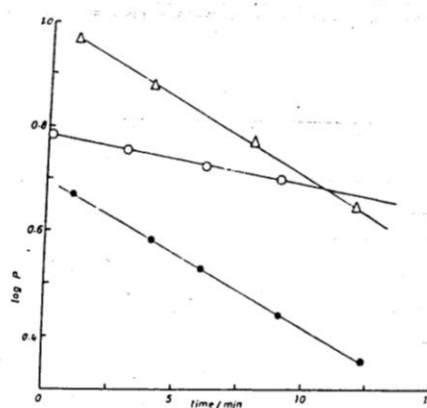


Figure 4. First-order plots for the adsorption of hydrazine on metal films of Fe ( $\bullet$ ) at 303 K, Ni ( $\circ$ ) at 373 K, and Cu ( $\Delta$ ) at 333 K. The hydrazine pressure ( $P$ ) was expressed in  $\text{N m}^{-2}$ .

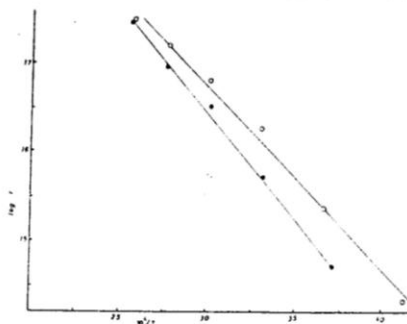


Figure 5. Arrhenius plots for the interaction of hydrazine with Fe, Ni, and Cu films. Symbols as in Figure 4. The rate of hydrazine adsorption was expressed in molecules  $\text{cm}^{-2} \text{ s}^{-1}$ .

TABLE IV: Activation Energy ( $E_a$ ) and the Preexponential Factor ( $\log A$ ) for Hydrazine Adsorption on Fe, Ni, and Cu Films over the Temperature Range 273–393 K

film	$E_a/\text{kJ mol}^{-1}$	$\log A^a$
Fe	$45.95 \pm 1.5$	$23.62 \pm 0.35$
Ni	$40.84 \pm 1.2$	$23.27 \pm 0.30$
Cu	$24.36 \pm 0.8$	$21.60 \pm 0.20$

<sup>a</sup>  $A$  in molecules  $\text{cm}^{-2} \text{ s}^{-1}$ .

Further hydrazine adsorption on Cu film continued above 303 K with dissociation; the gaseous products involved  $\text{NH}_3$ ,  $\text{N}_2$ , together with some  $\text{H}_2$  (Figure 3). The composition of the gas phase at several temperatures throughout hydrazine interaction with Cu film is given in Table III. The total gas pressure was found to increase while that of hydrazine decreased with time and temperature.

**Kinetics of Adsorption.** The rate of hydrazine adsorption depended directly on its pressure in the gas phase;<sup>12</sup> the pressure dependence was found to be unity with respect to each of the three metal films. Moreover, the logarithm of hydrazine pressure decreased linearly with time (Figure 4), in agreement with the

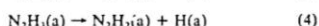
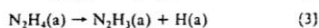
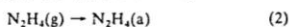
(12) A. Kant and W. J. McMahon, *J. Inorg. Nucl. Chem.*, **15**, 305 (1960).

derived value of the pressure dependence.

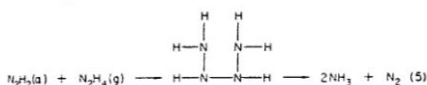
The activation energy ( $E_a$ ) of adsorption was constant for each film and was independent of the variations in the values of  $\theta$ . The value of  $E_a$  for each film was obtained from the plots of log rate ( $\log r$ ) vs.  $1/T$  where  $T$  is temperature in Kelvin (Figure 5). Table IV shows the values of  $E_a$  together with the values of the preexponential factors ( $A$ ) over the temperature range 273–393 K.

#### Discussion

**Adsorption and Decomposition.** The results of Table II show that  $\text{NH}_3$  was the major gaseous product of hydrazine adsorption and decomposition on Fe and Ni films at 243 K. There is considerable evidence in the literature<sup>2,12-14</sup> that the initial stage in the dissociation of hydrazine on the surface involves the rupture of N–H bonds ( $347.2 \text{ kJ mol}^{-1}$ ) in the following manner:

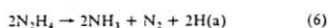


where (g) and (a) refer to the gaseous and the adsorbed species, respectively. This implies that the N–N bond ( $290.4 \text{ kJ mol}^{-1}$ ) is not broken in the process of  $\text{N}_2$  production due to the formation of a surface intermediate in which the N–N bond remains intact according to<sup>15</sup>



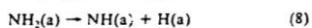
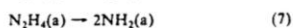
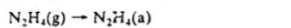
The adsorbed  $\text{N}_2\text{H}_2$  species (eq 4) react with gaseous hydrazine as in eq 5 to produce gaseous ammonia and nitrogen. A hydrogen abstraction step, involving two molecules of hydrazine in an activated complex, was originally postulated by Szwarc.<sup>16</sup> Thus, despite the relatively weaker N–N bond than the N–H of the hydrazine molecule, the N–N surface species may remain stable during the decomposition stage. This agrees with the general lack of correlation between bond strength and catalytic activity. The H/D isotope exchange of hydrocarbons in most cases exceeds isomerization reactions although the O–H bond is stronger than the C–C bond.<sup>2</sup>

The net results of adsorption and subsequent surface decomposition according to this mechanism, described by eq 2–5, may be written as



Molecular hydrogen may be formed by recombination of the mobile hydrogen adatoms (eq 3 and 4). Equation 5 gives a ratio of  $V_{\text{NH}_3}/V_{\text{N}_2}$  of 2 which agrees generally with the data of Table II particularly in the case of the Ni film.

With increasing extent of adsorption and temperature (>300 K) rupture of the N–N bond of the adsorbed hydrazine may occur forming amide and imide species on the surface.<sup>17,18</sup>



Further degradation of  $\text{NH}(\text{a})$  to  $\text{N}(\text{a}) + \text{H}(\text{a})$  is also possible

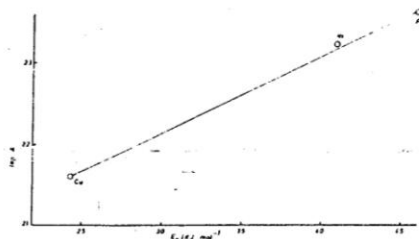
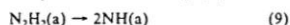


Figure 6. The relationship between  $\log A$  and  $E_a$  for the interaction of hydrazine with metal films of Fe, Ni, and Cu.

as such a transformation is known<sup>17</sup> energetically to be more favorable than that shown by eq 8. Surface imides may also be formed by further decomposition of surface  $\text{N}_2\text{H}_2$  species as<sup>18</sup>



Surface imides may undergo reaction with gaseous hydrazine to produce ammonia and nitrogen gases. Other reactions among various surface species are also possible.<sup>19,20</sup>

**Structure of the Surface Phase.** The results of Table II suggest that dissociative adsorption of hydrazine occurs on Fe and Ni films even at 243 K. If we assumed that the area covered by a chemisorbed hydrazine molecule is  $4/3$  that occupied by a krypton atom,<sup>21</sup> then the maximum value of  $\theta$  (0.6 on Fe and 0.73 on Ni) at 243 K probably correspond to coverages less than those required for the complete saturation of the surfaces. If we express the surface phase as  $\text{N}_x\text{H}_y$ , where  $x$  and  $y$  represent the number of nitrogen and hydrogen atoms, respectively, per adsorbed hydrazine molecule which are defined as

$$x = [2V_g - (2V_{\text{N}_2} + V_{\text{NH}_3})]/V_g \quad (10)$$

$$y = [4V_g - (2V_{\text{H}_2} + 3V_{\text{NH}_3})]/V_g \quad (11)$$

where  $V_g$ ,  $V_{\text{H}_2}$ , and  $V_{\text{NH}_3}$  are the volumes of nitrogen, hydrogen, and ammonia evolved, respectively, for the same surface coverage and composition, the values of  $x$  and  $y$  at 243 K are 1.61 and 3.28 for Fe ( $\theta = 0.6$ ) and 0.85 and 1.84 for Ni ( $\theta = 0.73$ ). These values indicate a greater extent of hydrazine adsorption and dissociation on Ni film at this temperature compared with Fe. Adsorption of hydrazine on Cu film at 243 K was likely to be molecular, in agreement with the data derived from ESCA.<sup>22</sup>

The surface phase on Fe film at temperatures 363–393 K corresponded to  $x = 1.0$  and  $y = 1.6$  when  $\theta$  approached 6.0. Such values may be accepted as proof of the existence of various proportions of such species as  $\text{N}_2\text{H}_2$ ,  $\text{NH}_2$ ,  $\text{NH}$ , as well as of some nitrides on the surface, and this may also account for the behavior of  $\text{N}_2$  liberation which is shown in Figure 2. The values of  $x$  and  $y$  in the surface phase  $\text{N}_x\text{H}_y$  on Ni were 0.15 and 0.31 at 363 K ( $\theta = 4.0$ ) and 0.07 and 0.20 at 393 K ( $\theta = 6.0$ ). Such low values of  $x$  and  $y$  suggest more extensive hydrazine dissociation on Ni than on Fe. The comparatively low values of  $x$  and  $y$  on Ni film at such temperatures indicate that the regeneration of the film surface, via the evolution of  $\text{NH}_3$ ,  $\text{N}_2$ , and  $\text{H}_2$  gases, is possible; a complete surface recovery, regardless of the physical alterations, may require temperatures higher than 393 K. A further point that may be derived from the low values of  $x$  and  $y$  on Ni is that the heat of adsorption of the product gases on Ni are likely to

(13) C. P. Seyer, Technical Report 69/10, Rocket Propulsion Establishment, Westcott, England, 1969.

(14) J. Block, *Z. Phys. Chem. (Frankfurt am Main)*, **138**, 1 (1972).

(15) Bernard J. Wood and H. Wise, *J. Catal.*, **39**, 471 (1975).

(16) M. Szwarc, *Proc. R. Soc. London, Ser. A*, **198**, 267 (1949).

(17) R. C. Cosser and F. C. Tompkins, *Trans. Faraday Soc.*, **67**, 526 (1971).

(18) M. H. Matloob and M. W. Roberts, *J. Chem. Res.*, **5**, 336 (1977).

(19) Ken-ichi Aika, T. Chhata, and A. Ozaki, *J. Catal.*, **19**, 140 (1970).

(20) R. C. A. Contaminard and F. C. Tompkins, *Trans. Faraday Soc.*, **67**, 545 (1971).

(21) J. M. Saleh, C. Kemball, and M. W. Roberts, *Trans. Faraday Soc.*, **57**, 1771 (1961).

(22) M. H. Matloob and M. W. Roberts, *J. Chem. Soc., Faraday Trans. 1*, **73**, 1393 (1977).

(23) Y. M. Dadiza and J. M. Saleh, *J. Chem. Soc., Faraday Trans. 1*, **68**, 269 (1972).

be somewhat lower than the corresponding values on Fe.

The evolution of  $\text{NH}_3$ ,  $\text{N}_2$ , and  $\text{H}_2$  gases subsequent to hydrazine adsorption on Cu film began at temperatures  $\geq 300$  K. The values of  $x$  and  $y$  for similar surface coverages were 0.95 and 1.87 at 363 K and 0.75 and 1.43 at 393 K. These values are higher than the corresponding values on Ni film and this may be attributed to the formation of strongly adsorbed species on the Cu surface, particularly at temperatures  $\leq 300$  K.

**Kinetics of Adsorption.** The kinetic data indicated the following:

1. The rate of hydrazine adsorption on each film was directly dependent on the pressure of the gaseous hydrazine.
2. The values of the activation energy ( $E_a$ ) of adsorption, as well as of the preexponential factor ( $A$ ), remained independent of the variations of  $\theta$ .
3. The results of Figure 6 suggest the operation of a compensation effect<sup>24-26</sup> in the hydrazine interaction with the metal

(24) S. A. Isa and J. M. Saleh, *J. Phys. Chem.*, **76**, 2530 (1972).

(25) M. K. Al-Noori and J. M. Saleh, *J. Chem. Soc., Faraday Trans. 1*, **69**, 2140 (1973).

(26) F. C. Constable, *Proc. R. Soc., London, Ser. A*, **108**, 355 (1925).

films over the temperature range 243–393 K. The sequence of the variations of  $E_a$  and  $\log A$  values in Figure 6 was  $\text{Cu} < \text{Ni} < \text{Fe}$ . Thus the activity of the films for hydrazine adsorption and decomposition could be arranged as  $\text{Cu} > \text{Ni} > \text{Fe}$ . The shortest Cu–Cu distance in a face-centered cubic structure is known<sup>27</sup> to be greater than the corresponding value for nickel. The chemisorbed hydrazine molecule will probably fit on such a copper spacing with only a very slight distortion of the Cu–N–N angle from its original value. This might suggest that the two-point attachment of the N–N of the hydrazine molecule might occur on copper without a significant strain. Thus, the geometric requirements for appropriate adsorption of hydrazine are probably more satisfied on Cu than on Ni. Iron with a body-centered cubic structure and of similar atomic radius<sup>27</sup> to Ni is shown from Figure 6 to be somewhat less active than Ni for hydrazine adsorption and decomposition.

Registry No.  $\text{N}_2\text{H}_4$ , 302-01-2; Cu, 7440-50-8; Fe, 7439-89-6; Ni, 7440-02-0.

(27) R. H. Griffith and J. D. F. Marsh, "Contact Catalysis", Oxford University Press, London, 1957, pp 135–145.

## Time-Resolved Measurements of the Fluorescence of Rhodamine B on Semiconductor and Glass Surfaces

Y. Liang and A. M. Ponte Goncalves\*

Department of Chemistry, Temple University, Philadelphia, Pennsylvania 19122  
(Received: September 24, 1984)

Time-correlated single-photon counting was used to investigate the fluorescence decay of rhodamine B at semiconductor–water and glass–water interfaces. All decays could be fit by the sum of two exponentials with lifetimes  $\tau_1$  (short) and  $\tau_2$  (long). At very low dye concentrations in solution ( $10^{-7}$  M)  $\tau_1 = 0.41$  ns and  $\tau_2 = 1.4$  ns for semiconductors (tin oxide and indium oxide), and  $\tau_1 = 0.68$  ns and  $\tau_2 = 2.6$  ns for glass. Experiments on dry surfaces prepared with  $10^{-7}$  M rhodamine B solutions gave  $\tau_1$  values similar to those obtained for surface–solution samples, but  $\tau_2 = 3.1$  ns with both glass and semiconductor surfaces. We assign  $\tau_1$  to molecules which are capable of excited-state electron transfer to the semiconductors or to glass, and  $\tau_2$  to those which are not. Progressively shorter  $\tau_1$  values measured for  $\text{SnO}_2$  with increasing dye concentrations are attributed to the effect of energy-transfer quenching. Treatment of  $\text{SnO}_2$  surfaces in 1 M KCl solutions at pH 13 (reported to reduce the photocurrent yield by two orders of magnitude) had no effect on  $\tau_1$ . No changes in  $\tau_1$  which could be attributed to enhanced electron transfer were found with supersensitizers (thiourea and hydroquinone), which are known to increase the photocurrent yield by as much as one order of magnitude.

### Introduction

Electron transfer from photoexcited states of adsorbed dye molecules into large band-gap n-type semiconductors has long been assumed, with some justification, to be very fast and thus to take place with quantum efficiency near unity.<sup>1-3</sup> However, photocurrent yields,  $\phi$ , measured for dye-sensitized semiconductor–electrolyte cells are often on the order of  $10^{-2}$  or less.<sup>1-4</sup> The low  $\phi$  values have been attributed to trapping of the injected electrons near the surface and subsequent recombination with the oxidized dye molecules,  $D^+$ . A number of indirect attempts were made to obtain the rate constant for the primary electron-transfer step,  $k_e$ , and values on the order of  $10^{10}$  s<sup>-1</sup> were generally estimated.<sup>3-5</sup> These efforts were hindered by the fact that energy-transfer

quenching of the dye excited state,  $D^*$ , cannot be discounted at the relatively high surface coverages commonly used. We have recently performed fluorescence quantum yield measurements<sup>6</sup> with rhodamine B on tin-doped indium oxide surfaces at progressively lower surface coverages and obtained  $k_e = 1.2 \times 10^{10}$  s<sup>-1</sup>. However, the considerable uncertainties associated with fluorescence quantum yield measurements, especially for adsorbed dyes,<sup>6</sup> make reliable estimates of  $k_e$  rather difficult. Our early attempt<sup>7</sup> at a more direct determination of  $k_e$  through the dye fluorescence lifetime succeeded only in showing that energy-transfer quenching plays a dominant role at high surface coverage. The relatively low sensitivity of the streak camera system used in those experiments did not allow us to perform measurements at the very low surface coverage required for negligible energy-transfer quenching. In order to overcome this obstacle, we have used a time-correlated single-photon counting technique to obtain the time-resolved fluorescence of rhodamine B at semiconductor–water and glass–water interfaces, down to very low surface

(1) H. Gerischer and F. Willig, *Top. Current Chem.*, **61**, 31 (1976).

(2) H. Gerischer, M. T. Spitzer, and F. Willig in "Proceedings of the Third Symposium on Electrode Processes, 1979", S. Bruckenstein, Ed., The Electrochemical Society, Princeton, NJ, 1980, p 115.

(3) M. Spitzer, M. Lubke, and H. Gerischer, *Chem. Phys. Lett.*, **56**, 577 (1978).

(4) T. Yamase, H. Gerischer, M. Lubke, and B. Pettinger, *Ber. Bunsenges. Phys. Chem.*, **82**, 1041 (1978).

(5) W. Arden and P. Fromherz, *J. Electrochem. Soc.*, **127**, 370 (1980); *Ber. Bunsenges. Phys. Chem.*, **84**, 1045 (1980).

(6) Y. Liang, P. F. Moy, J. A. Poole, and A. M. Ponte Goncalves, *J. Phys. Chem.*, **88**, 2451 (1984).

(7) Y. Liang, A. M. Ponte Goncalves, and D. K. Negus, *J. Phys. Chem.*, **87**, 1 (1983).